Focusing of Surface Waves

Gerardo Ruiz-Chavarria, Michael Le Bars and Patrice Le Gal

Abstract In this chapter we present some original experimental results of the process of focusing of surface waves in a fluid. To this end, monochromatic waves of frequencies in the range 5–15 Hz are produced in a water layer of 10 cm depth using a parabolic wave maker. Experiments remain in the deep water approximation and both gravity and surface tension influence the evolution of waves. We find that, as in optics, the wave field exhibits phenomena such as diffraction, interference and the presence of two caustics intersecting at one point and forming a cusp. To investigate the properties of surface waves, the synthetic Schlieren method is used. Nonlinear behavior emerges during the process of focusing even for small amplitude waves. For example the peak amplitudes are more pronounced that the amplitude of the troughs. Some non expected results emerge from our experiments. The first is that the position of the maximum amplitude of the wave is dependent on the amplitude of the initial parabolic wave front, but in any case, is always in the vicinity of the origin of Huygens' cusp. Second, the predictions for linear waves are only in partial agreement with our experimental data. And finally, due to the fact that the ratio of the size of wave maker to the wavelength does not tend to infinity some finite size effects are observed.

G. Ruiz-Chavarria (✉)
Facultad de Ciencias, Universidad Nacional Autónoma de México,
Ciudad Universitaria,
04510 Mexico, México D.F., Mexico
e-mail: gruiz@unam.mx

M. L. Bars · P. L. Gal
Institut de Recherche sur les Phénomènes Hors Equilibre, UMR 7342,
CNRS - Aix-Marseille Université 49 rue F. Joliot Curie,
13384 Marseille, Cédex 13, France
e-mail: lebars@irphe.univ-mrs.fr

P. L. Gal
e-mail: legal@irphe.univ-mrs.fr

J. Klapp and A. Medina (eds.), *Experimental and Computational Fluid Mechanics*, Environmental Science and Engineering, DOI: 10.1007/978-3-319-00116-6_27,

1 Introduction

In the theory of waves, the caustics are surfaces that separate illuminated regions from shaded regions. Geometrical optics establishes that in the illuminated region several rays reach each point, while in the shaded region no rays are present. The same theory predicts that the amplitude of the wave goes to infinity along the caustic. In reality this behavior does not hold, because the ray theory is only an approximation coming from geometrical optics forgetting about the wave properties. However, the behavior of a wave in the vicinity of a caustic has been investigated in the past (Paris and Kaminski 2001; Lewis et al. 1967; Stamnes and Spjelkavik 1983) for two rays superimposition. In this case, the wave field can be described in terms of the Airy function Ai(x). This function has an oscillating behavior for $x < 0$, while for $x > 0$ the amplitude has an exponential smooth behavior. In fact, the problem we present in this manuscript cannot be described only in terms of Airy function because inside the cusp the wave field is the result of the superposition of three rays. The method proposed by Pearcey (1946) must be used in this case instead of the classical theory. In surface waves, a field with a Huygens' cusp can be produced with a parabolic wave maker (Pomeau (1991), see Fig. 1). The initial wavefront is described by the equation

$$y_0 = ax_0^2 \tag{1}$$

A ray starting at the parabola of equation $y_0 = ax_0^2$ moves in a direction perpendicular to it, i. e. in a direction given by the normal vector $\hat{n}$ in the point: (x_0, y_0):

$$\hat{n} = \frac{(-2ax_0, 1)}{\sqrt{1 + 4a^2x_0^2}} \tag{2}$$

As the wave travels, its amplitude grows by focusing according to the following relation:

$$A = A_0\sqrt{\frac{\rho}{\rho - d}} \tag{3}$$

where A_0 is the initial amplitude, d is the distance traveled by the ray and $\rho = \frac{1}{K}$ is the inverse of the curvature of the parabola at the starting point, which in actual case is:

$$K = \frac{y_0''}{(1 + y_0'^2)^{3/2}} = \frac{2a}{(1 + 4a^2x_0^2)^{3/2}} \tag{4}$$

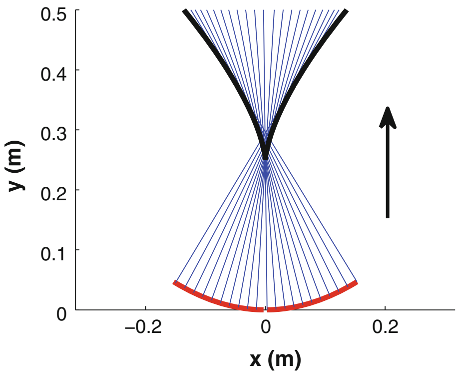

Fig. 1 Parabolic wave maker (*red line*). The equation of the curve is $y_0 = ax_0^2$. According to geometrical optics a ray starts at the parabola and moves in a direction normal to the curve (*blue lines*). In the figure, the Huygens' cusp is plotted as the *black line*. The *arrow* in the figure indicates the direction of propagation of waves

The space where the wave progresses is divided in two regions. In the first one, which is in contact with the parabolic wave maker, only one ray passes through each point. Far away a second region emerges; it is characterized by the fact that three rays reach each point. The curve separating both regions is the union of two caustics. One way to obtain the analytical expression of the caustics is to determine the limit of the region where only one real root exists for x_0 in the equation of a ray in parametric form $(x, y) = (x_0, y_0) + \hat{n}d$. An alternative method is to use the property that in the ray theory a caustic is the locus where the amplitude becomes infinite. This happens for $d = \rho$ (Eq. 3). That is:

$$(x, y) = (x_0, ax_0^2) + \hat{n}\rho = (-4a^2x_0^3, \frac{1}{2a} + 3ax_0^2) \tag{5}$$

The analytical expression for caustics can be obtained if we combine both components of this vector equation and eliminate x_0. This procedure leads to the following equation

$$x = \pm\frac{4\sqrt{a}}{3\sqrt{3}}(y - \frac{1}{2a})^{3/2} \tag{6}$$

The last equation has a cusp singularity at $(0, \frac{1}{2a})$ where both caustics intersect. Far from this point, the characteristics of the wave can be deduced using the method of the stationary phase. Near the cusp, the amplitude $h(x, y)$ of the surface wave can be calculated by the diffraction integral (Pearcey 1946; Paris and Kaminski 2001), which is an approximate solution of the wave equation:

$$h(x, y) = \int_{-\infty}^{+\infty} \frac{dx_0}{cos(\theta(x_0))} \frac{exp(ikd(x_0, x, y))}{\sqrt{d(x_0, x, y)}} \tag{7}$$

where $\theta(x_0)$ is the angle between the tangent to parabola at point (x_0, y_0) and the x axis. We assume that $cos(\theta(x_0)) \approx 1$. Interest is pointed out in the solution around the singular point $(0, \frac{1}{2a})$. For this purpose we made a Taylor expansion of $d(x_0, x, y)$ about this point. At first order we obtain:

$$d(x_0, x, y) \approx R + \frac{1}{2R}\left(a^2 x_0^4 + 2a\left(\frac{1}{2a} - y\right)x_0^2 - 2xx_0\right) \tag{8}$$

where $R = \frac{1}{2a}$. This expression is used only in the exponential term because $kd(x_0, x, y)$ is a rapidly varying variable and in the denominator we made the approximation that $d(x_0, x, y) \approx R$. The diffraction integral is then approximated by:

$$h(x, y) = \frac{exp(ikR)}{\sqrt{R}} \int_{-\infty}^{+\infty} exp\left(\frac{ik}{2R}\left[a^2 x_0^4 + 2a(\frac{1}{2a} - y)x_0^2 - 2xx_0\right]\right) dx_0 \tag{9}$$

Let us make the following change of variable $x_0 = \left(\frac{2R}{ka^2}\right)^{1/4} t$ and define two quantities $U = 2\left(\frac{k}{2R}\right)^{1/2}(\frac{1}{2a} - y)$ and $V = -\frac{2}{\sqrt{a}}\left(\frac{k}{2R}\right)^{3/4} x$.

Then we recover the Pearcey integral (Pearcey 1946; Berry 1992) for a linear wave in the vicinity of a cusp:

$$h(x, y) = \frac{k}{i2\pi} \frac{exp(ikR)}{\sqrt{R}} \left(\frac{2R}{ka^2}\right)^{1/4} \int_{-\infty}^{+\infty} exp\left(i\left[t^4 + Ut^2 + Vt\right]\right) dt \tag{10}$$

In the precedent equation the integral extends from $-\infty$ to $+\infty$. However, even if in a surface wave field λ is usually smaller than the length R , the ratio $\frac{R}{\lambda}$ does not go to infinity as in the case for light and the integral in Eq. 10 must be calculated for a finite interval. In Fig. 2 we show the envelope of the amplitude along the axis of symmetry x = 0 for a wave of frequency ν = 10 Hz (black line). We assume that the surface is excited with a parabolic wave maker whose parameter a is 0.02 cm^{-1} and that extends in the interval $-15\,cm < x_0 < 15\,cm$. The curve is obtained from Eq. 10, but the integration is performed over a finite interval. For comparison we have also included the curve when the integration is made in an infinite domain $-\infty < t < \infty$ (blue line), the envelope calculated from a numerical solution of the wave equation (magenta line) (Ruiz-Chavarria et al. (2011)) and the asymptotic behavior resulting from the method of stationary phase (dashed red line). In all cases

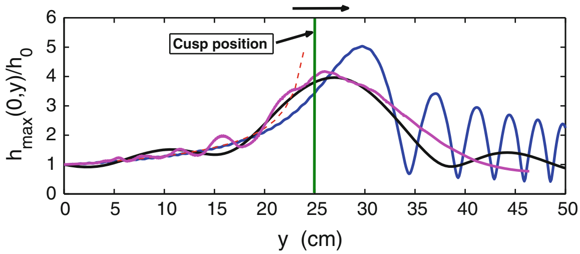

Fig. 2 Envelope of the wave amplitude along the axis of symmetry (*black line*) according to the diffraction integral calculated on a finite interval. h_0 is the amplitude at the wave maker. For comparison we also plot the curve when the integral extends from $-\infty$ to $+\infty$ (*blue line*), the curve obtained from the linear wave equation (*magenta line*) and the asymptotic behavior given by the ray theory (*red line*). In the last case, amplitude is proportional to $\sqrt{\frac{1}{(\frac{1}{2a}-y)}}$ and diverges at the cusp. The theoretical position of the cusp is indicated with the *vertical green line*

the initial amplitude A_0 is set to 1. As can be seen, the diffraction theory (both for finite and infinite integration domain) and the solution of the wave equation predict that the maximum amplitude happens further than the Huygens' cusp (on the right of the theoretical cusp position on the figure) . Moreover, the diffraction theory for a finite integration interval and the solution of the linear wave equation predict the same result for the position and the value of the maximum amplitude. On the other hand the Pearcey integral predicts the existence of oscillations of the envelope to the right of the cusp, whereas the solution of wave equation exhibits a monotonic decrease of the wave amplitude.

2 Experimental Setup

Experiments were carried out in a basin of size 120 cm × 50 cm × 15 cm made in plexiglass (see Fig. 3). The basin is filled with water up to a level of 10 cm. In order to produce the wave field the parabolic wave maker is connected to a mechanical vibrator. In all cases a monochromatic wave is produced, with a frequency between 5 and 15 Hz.

The shape of the free surface is determined with the method known as synthetic Schlieren (Moisy et al. 2009). This procedure is based on the fact that a change in the slope of the liquid-air interface causes a change in the direction of the light rays that cross this surface. Then, if a pattern of dots is placed at the bottom of the liquid layer, there is an apparent displacement of them when the free surface is deformed. The synthetic Schlieren method works well when the slope of the liquid-gas interface is small. In our case, the initial amplitude (at the edge of the parabolic wave maker) is of the order of tens of microns whereas the maximum amplitudes attained during focusing is about 150 μm. If we consider that the smallest wavelength measured in the

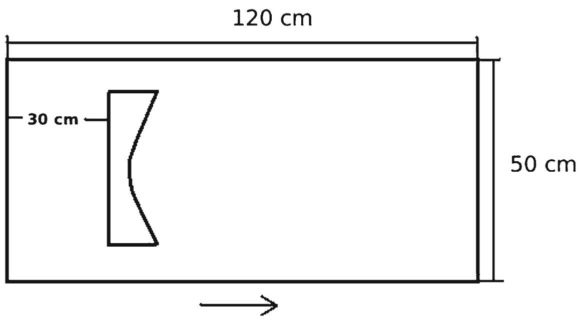

Fig. 3 The experiments of wave focusing were made in a plexiglass basin. The wave maker was colocated approximately to 30 cm away from the left border. Waves progresses from left to the right as indicated by the *arrow*. Frequencies in the mechanical vibrator moving the wave maker lies in the range 5–15 Hz. In most experiments camera is at a distance of 1 m from the free surface

experiments is 1.5 cm, the maximum value of the ratio of amplitude to wavelength is 0.15/15 = 0.01. Consequently the slopes remain small and the validity of the measurement method is guaranteed. Higher slopes could produce a failure of the method because the crossing of the light rays when travel from the bottom to the free surface.

The method uses a video camera to record the spatio-temporal evolution of the surface elevation. In order to have a good resolution we used a high definition camera, with an image size of 1,920 × 1,080 pixels. The area covered by a frame is 18.5 cm × 10.4 cm, so the conversion factor between pixels and length is 103.8 pixel / cm. To determine the wave features we printed in a paper sheet a pattern of dots randomly distributed. This sheet is placed at the bottom of the basin. A snapshot of the dot pattern is taken when the free surface is at rest (hereafter called the reference image). In a second step images of are taken when a surface wave passes. Apparent displacement is measured with a PIV software. As usually done in Particle Image Velocimetry the pictures are divided into a set of cells having a size of 32 × 32 pixels. The number of cells in each direction is 128. In order to reconstruct the form of the water-air interface we recall the relation between the apparent displacement δr and the gradient of the free surface h (Moisy et al. 2009):

$$\nabla h = -\frac{\delta \mathbf{r}}{h^*} \tag{11}$$

where $\frac{1}{h^*} = \frac{1}{\alpha h_p} - \frac{1}{H}$. H is the distance from the camera to the bottom of the fluid layer, h_p is the thickness of the fluid and $\alpha = 1 - n'/n$ (n' and n are the refraction indices of the gas and liquid respectively). The reconstruction of the topography of the free surface can be done by integration of Eq. 11. The system of equation is overdetermined and a least square routine is used to calculate h(x, y, t).

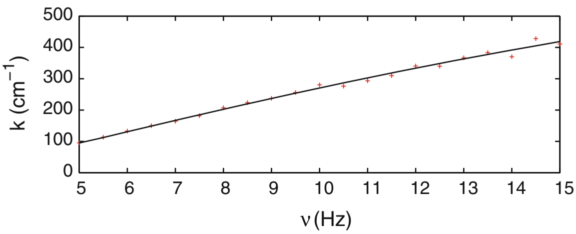

Fig. 4 Dispersion relation for a plane wave (wavenumber versus frequency). The determination of the wavelength was done with the method of periodograms. In the same figure the curve obtained from Eq. 12 has been also included. It can be observed a good agreement between the theory and experiments, which is a test of the validity of the synthetic Schlieren method

3 Results

The dispersion relation for a surface wave in a liquid is given by the following equation (Elmore and Heald 1969) :

$$\omega^2 = \left(gk + \frac{\sigma k^3}{\rho}\right) \tanh(\mathrm{kh}) \tag{12}$$

where $\omega = 2\pi\nu$ is the pulsation of waves, $k = \frac{2\pi}{\lambda}$ is the wavenumber, σ is the surface tension coefficient of the liquid and ρ is the density of the fluid. The first experiment we made was the measurement of λ for different frequencies. To this end, we have used a 30 cm long plane wave maker. In order to have a precise estimate of λ, we use the procedure based on periodograms. Figure 4 shows the graph of the wavenumber k versus frequency. For comparison we have included the prediction given by Eq. 12. The agreement is very good implying that the synthetic Schlieren method reproduces well the properties of waves in the system under study.

With regard to the process of focusing, measurements of the topography of the free surface were made. The liquid-gas interface was excited with the parabolic wave maker.. Measurements were carried out in a region between $15 < y < 45$ and $-8 < x < 8$. The diffraction theory predicts that the maximum amplitude is attained inside this region. Wave fronts-initially convergent- become divergent after passing the origin of Huygens' cusp. In Fig. 5 we present two graphs of the free surface shape versus (x, y) for a wave of frequency $f = 10$ Hz corresponding to a wavelength $\lambda = 2.32$ cm. To the right of each figure there is a scale which gives the color to the value of the surface deformation h. As we can see in Fig. 5a (which covers the interval $15 < y < 25$) the focusing leads to an increase of the amplitude when wave moves from left to the right. In Fig. 5b the topography of the free surface versus the (x, y) coordinates, is plotted for the interval $25 < y < 35$. In the same figure, the Huygens' cusp is also plotted as a dashed line. The figure exhibits the change from a convergent (left side) to a divergent (right side) wave field. As expected, the

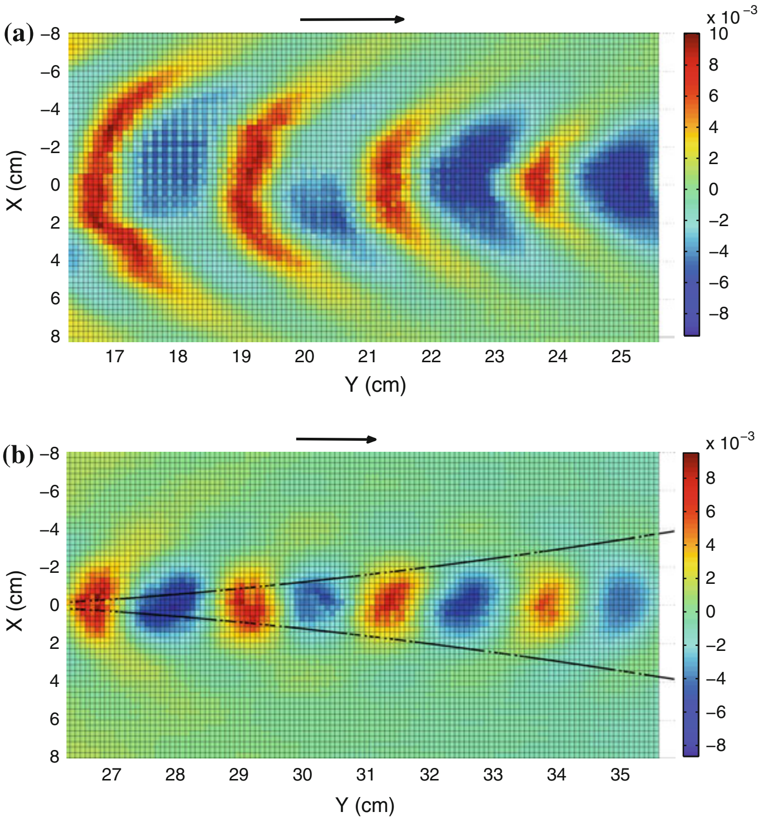

Fig. 5 Topography of free surface h in the plane (x, y) of a wave produced by a parabolic wave maker. Amplitude is proportional to the color intensity. *Red* stands for positive values and *blue* stands for negative values. The vibrator was driven at a frequency of 10 Hz, which corresponds to a wavelength $\lambda = 2.32$ cm. **a** free surface in the range $15 < y < 25$. The focusing leads to an increase in amplitude of the wave. **b** free surface in the range $25 < y < 35$. The wave amplitude reaches a maximum and then there is a decrease in amplitude and an inversion in the wavefront is observed to the right

maximum amplitude is reached along the axis of symmetry after the wave traverses the cusp. In Fig. 6 we present a snapshot of the wave field for $35 < y < 45$. In this region, the wave is divergent and consequently the amplitude decreases as the wave travels. The amplitude of the wave does not exhibit oscillations in this region as predicted by Eq, 10, because away from the cusp interference does not happen.

A most appropriate way to exhibit the focusing is by means of the envelope of the wave along the axis of symmetry. The observed behavior is the combination of nonlinearities and a finite size effect. For a linear wave, the diffraction theory predicts that, when $\frac{R}{\lambda}$ approaches to infinity the maximum amplitude occurs at y = 28.6. Taking into account that $\frac{R}{\lambda}$ has a finite value, the maximum amplitude for a wave of frequency ν = 10 Hz should occur at y = 25.5 according to the linear wave

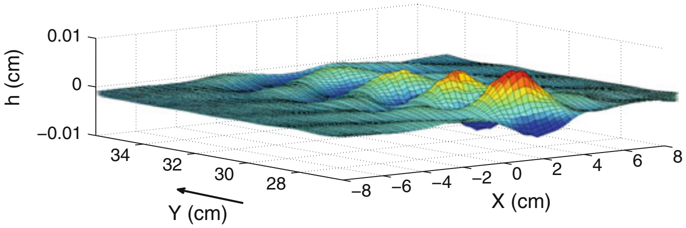

Fig. 6 Topography of the free surface h in the plane (x, y) of a wave produced by a parabolic wave maker ($a = 0.02\,cm^{-1}$). The vibrator was driven at a frequency of 10 Hz, which corresponds to a wavelength $\lambda = 2.32$ cm. This figure clearly shows the decrease in amplitude as a function of y away from cusp. The amplitude becomes proportional to $\sqrt{\frac{1}{y-\frac{1}{2a}}}$ as predicted by the theory of linear waves

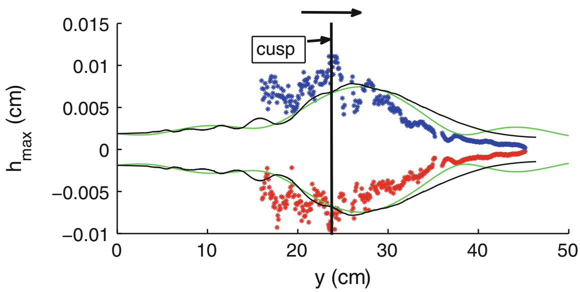

Fig. 7 Envelope of the wave along the axis of symmetry x = 0. The surface of the fluid is excited with a frequency of 10 Hz, which corresponds to a wavelength $\lambda = 2.32$ cm. The positive and negative branches of the envelope have a small asymmetry. This is a signature of the appearance of nonlinearities. Otherwise, maximum amplitude is reached near the origin of cusp. For comparison, the prediction of diffraction theory is also included (*green line*) and the solution of the wave equation (*black line*). Amplitudes attained by the waves are greater than the prediction of the linear theory of waves

theory In experiments we have found that position of maximum is dependent of the initial amplitude A_0 of the wave front. Figure 7 shows the envelope of the wave on the axis of symmetry for an initial amplitude of $\approx 20\ \mu$m . In the same figure the curves of diffraction theory (green line) and the solution of wave equation (black line) are included. First, the positive and negative branches of the envelope have a small asymmetry and in this sense non linearities are weak. On the other hand the position of maximum is located to the left of black and red curves. Finally, the behavior of the envelope to the right of the figure shows a more pronounced decrease with respect to the predictions of the diffraction and the linear wave theories. For a greater value of the initial amplitude A_0 the experimental data show a shift of the position of the maximun to the right. This behavior can be observed in Fig. 8, in which the envelope is plotted for $A_0 \approx 25\ \mu$m. Under these circumstances the maximum amplitude is approximately that predicted by the linear theory. Concerning the behavior away from the cusp, experimental data and models show a similar trend. And finally the

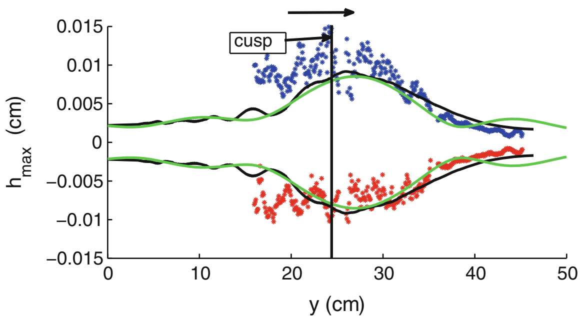

Fig. 8 Envelope of the wave along the axis of symmetry. The surface of the fluid is excited with a frequency of 10 Hz, which corresponds to a wavelength $\lambda = 2.32$ cm. The position of maximum is shifted to the right with respect the previous figure, having a value close to the prediction by linear theory. Otherwise, positive and negative branches of the envelope become clearly asymmetric, which is a signature of the non linear effects. For comparison, the prediction of diffraction theory (*green line*) and the solution of the wave equation (*black line*) are also included

positive and negative branches of the envelope become clearly different, indicating that non linearities are relevant as expected for larger amplitude waves.

4 Conclusions

In this chapter we investigated the focusing of surface waves in water by the synthetic Schlieren method. For this purpose the liquid-gas interface was excited with a parabolic wave maker. Although the waves produced in experiments have small amplitude the non linear effects are important in the vicinity of the Huygens' cusp. In this respect, we have observed that the growth of peaks is greater than that predicted by the linear theory. In the same sense the positive and negative branches of the envelope become asymmetric as the initial amplitude grows. Another important result is that away from the Huygens cusp the wave field becomes divergent and non linearities stay weak in this region.

The experimental results presented here are the first step in the study of non linear waves near a cusped caustic, which is at present an open subject. Some new phenomena non present in linear waves will be investigated in the future. This is for instance the case of wave breaking that can be induced by the focussing process (Tejerina-Risso and Le Gal (2012)).

Acknowledgments G. Ruiz-Chavarria acknowledges DGAPA-UNAM by support for a sabbatical period at IRPHE between september 2010 and august 2011. Additionally the same author acknowledges support by DGAPA-UNAM under project 116312, "Vorticidad y ondas no lineales en fluidos"

References

Paris RB, Kaminski D (2001) Asymptotics and mellin-barnes integrals. Cambridge University Press. Cambridge, pp 442

Lewis RM, Bleistein N, Ludwig D (1967) Uniform asymptotic theory of creeping waves. Commun Pure Appl Math 20:295–328

Stamnes JJ, Spjelkavik B (1983) Evaluation of the field near a cusp of a caustic. Optica Acta: Int J Opt 30:1331–1358

Pearcey T (1946) The structure of an electromagnetic field in the neighbourhood of a cusp of a caustic. Phil Mag 37:311–317

Pomeau Y (1991) Caustics of nonlinear waves and related questions. Europhys Lett 11:713–718 and private communication

Berry M (1992) Rays, wavefronts and phase: a picture book of cusps in Huygens' Principle 1690–1990: theory and applications. Elsevier 299:97–111

Ruiz-Chavarria, G, Le Bars M, Le Gal P, Pomeau Y (2011) Focalisation d'ondes de surface et déferlement. In: Proceedings of the 20eme congres francais de mecanique. Besancon (2011) Art. p 552

Moisy F, Rabaud M, Salsac K (2009) A synthetic Schlieren method for the measurement of the topography of a liquid interface. Exp Fluids 46:1021–1036

Elmore WC, Heald MA (1969) Physics of waves. McGraw Hill, New York, p 477

Tejerina-Risso J, Le Gal P (2012) Around the cusp singularity and the breaking of waves. In: Proceedings of the conference "Water is in the Air", Marseille, 25–26 June 2012